

# ***Toward a Loss-Driven Earthquake Early Warning and Rapid Response System for Kyrgyzstan (Central Asia)***

**by M. Pittore, D. Bindi, J. Stankiewicz, A. Oth, M. Wieland, T. Boxberger, and S. Parolai**

## **INTRODUCTION**

Over the last decade, increasing attention has been paid by the international community to the topic of earthquake early warning (EEW) systems, as a viable solution to protect specific hazard-prone targets (major cities or critical infrastructure) against harmful seismic events. The aim of the EEW system is to detect the occurrence of an earthquake and to determine its relevant characteristics (such as location and magnitude) early enough to predict the ground shaking at the target site before the *S*-wave arrival. Possible emergency protocols that can be activated upon event detection range from slowing down or stopping rail traffic (Nakamura, 2004; Horiuchi *et al.*, 2005; Espinosa-Aranda *et al.*, 2011), safely shutting down or activating protective measure of critical infrastructures such as nuclear power plants (Saita *et al.*, 2008), to broadcasting alerts to the general public (Wenzel and Lungu, 2000; Lee and Espinosa-Aranda, 2002; Allen and Kanamori, 2003; Horiuchi *et al.*, 2005; Wu *et al.*, 2007). Only few systems have been actually implemented and are currently operational. Examples of regional applications are the systems operating in California, Japan, and Taiwan, whereas targeted systems have been developed, for instance, in Mexico, Irpinia (Italy), and Vrancea (Romania). We refer the interested readers to the comprehensive references in Wenzel and Zschau (2014).

Despite the potential benefits of EEW system, several factors so far hindered their widespread application especially in economically developing countries. When the distance between the seismic sources and the exposed target is too short for instance, or there is no technological infrastructure supporting real-time, automatic operations, the information provided by the EEW system cannot be exploited for pre-event actions. In these cases, which occur remarkably often in many seismic regions, the level of ground shaking predicted by the system can still be used as input for generating risk scenarios in near real time, leading to the generalized concept of earthquake early warning and rapid response systems (EEWRRSs). Different approaches can be implemented for earthquake loss modeling depending on the specific task (see Astoul *et al.*, 2013 and references therein). Examples include probabilistic methods selecting a maximum probable loss scenario with respect to

a stochastic event portfolio (e.g., Robinson *et al.*, 2006) and deterministic methods in which a specific event scenario is considered (e.g., Sousa *et al.*, 2004). Several systems have been proposed and implemented in the last decade, such as KOERILOSS (Erdik *et al.*, 2003), HAZUS (Kircher *et al.*, 2006), PAGER (Wald *et al.*, 2010), and SELINA (Molina *et al.*, 2010).

In this study, we describe the main requirements that an EEWRRS should match to be a viable complement to other disaster risk reduction strategies, particularly in economically developing countries, that have received little attention in this context thus far. The aim of the proposed solution is thus not to compete with these elaborate systems but rather to devise an optimal strategy for EEWRRS in the many countries suffering from limited resources.

The system embeds a risk estimation module that extracts from a portfolio of precomputed scenarios those matching the characterization of the event detected by an optimized real-time monitoring network with local and regional components.

The proposed concept system can be applied to many economically developing countries, where civil protection authorities would greatly benefit from prompt and reliable loss estimations for mitigating earthquakes' consequences. In particular, an exemplification of this system is discussed for Bishkek, Kyrgyz Republic, and could be extended to most of the other Central Asian countries.

## **REQUIREMENTS FOR EARLY WARNING AND RAPID RESPONSE SYSTEMS IN CENTRAL ASIA**

To provide reliable and affordable solutions for seismic risk mitigation and resilience improvement in Central Asia, the following requirements have been identified for the proposed EEWRRS:

*Target-based.* Priority targets should be selected (e.g., major cities or critical infrastructure), also considering the expected benefits of the system (see following requirements). The size and geometry of the monitoring network should be optimized by considering up-to-date hazard models to provide useful lead times.

*Dual-use.* Dual-use refers to the combination of early warning and rapid response use patterns in a single, hybrid system

that can fully exploit the investment in monitoring infrastructures (both regional and on-site) by providing both timely warning and response-focused real-time information. In Central Asia, some of the capitals and major cities (e.g., Bishkek, Almaty, Tashkent, and Dushanbe) are threatened both by close-range and long-range (and higher magnitude) events. The on-site EEW components would focus mainly on loss estimation and rapid response, whereas a regional monitoring infrastructure would provide a timely warning for long-range events. Simulations based on hazard models can be used to validate this assumption (see [Data Layer](#) section).

*Loss-driven.* Assessment of seismic risk should always be the bottom line of the EEWRRS development. Provision of real-time estimates of expected consequences can reduce response times and better focus emergency management, thus increasing the response and recovery capacities. Risk-related information must be kept up-to-date and validated to be useful upon the occurrence of an event. Use of scenario modeling and simulation is proposed to estimate expected consequences. A comprehensive loss assessment is also the basis for cost-benefit analyses, which should be used to trim the system's operational parameters (e.g., warning activation thresholds), to plan and prioritize mitigation and prevention measures and to improve risk communication to a wide range of stakeholders.

*Technologically viable.* The complexity of the system and its technological requirements should be carefully considered to provide functional and economically viable solutions, suit-

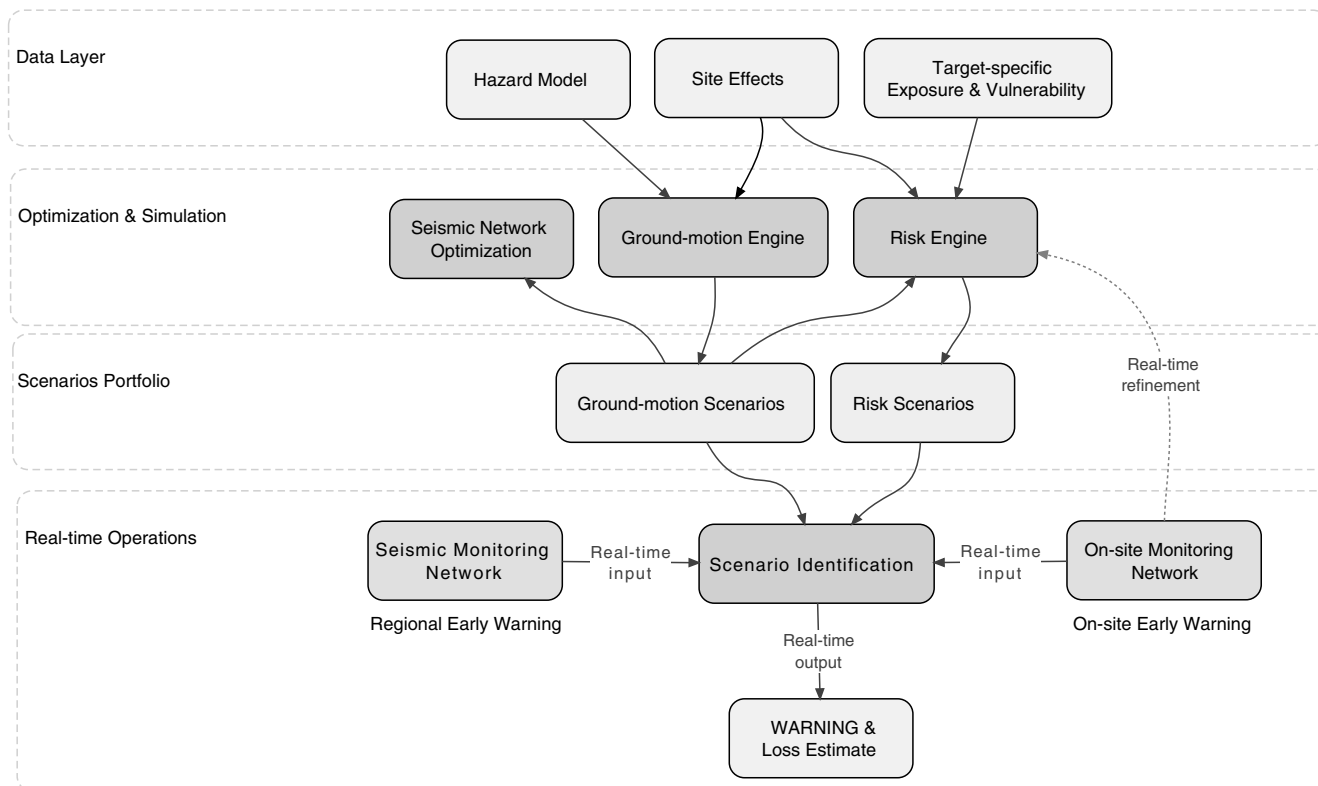
able to countries, like those in Central Asia, with little resources available. Fault tolerance should be implemented within a careful design of the architecture and the components of the system to not inflate the costs and to ensure long-term sustainability.

*Uncertainty-aware.* Uncertainty is a common factor underneath all the mentioned requirements. Inaccurate prediction of the incoming strong motion can result in false alarm costs or, even worse, in a failure of the alerting system to mitigate the consequence of an earthquake. In rapid response applications, poor characterization of the events can negatively affect emergency response. Uncertain exposure and vulnerability models can heavily impact the reliability of the loss estimates, jeopardizing the prevention and mitigation of the expected consequences.

## PROPOSED CONCEPT

Considering the requirements mentioned above, and with the specific goal of deploying such systems in Central Asia, an EEWRRS architecture is proposed, based on the groundwork introduced by [Picozzi et al. \(2012\)](#) and [Pittore et al. \(2012\)](#). We exemplify our approach on Bishkek, the capital of Kyrgyzstan, being representative of many large cities in the same region.

The system is basically composed of a real time and an off-line macroblock (see outline in [Fig. 1](#)). The offline macroblock includes the data input, that is, the information constraining



▲ **Figure 1.** Outline of proposed system architecture's components. An aggregation of the components with similar scope is shown, based on several macroblocks (discontinuous lines, labels on the left).

hazard and risk modules, and the data output layers (both ground motion and loss scenarios obtained by simulation). A further layer in the offline block includes all the simulation and optimization processing stages, which take the input from the data layer and produce the scenarios. All simulations are conducted offline. The seismic network optimization component is used mainly in the system's design phase to find the optimal placement of the monitoring network, whereas the simulation engines provide the simulated ground motion and loss scenarios to the scenario identification component.

The real-time block includes a network of monitoring sensors, both on-site and regionally distributed. A dynamic refinement of simulated scenarios is envisaged based upon the input from on-site monitoring network. The main task of the scenario identification component is to detect the event and to predict its impact by identifying the most suitable loss scenarios in the available portfolio.

The main components providing event detection and consequence estimation will be discussed in the following sections, according to the thematic subdivision sketched in Figure 1. Further necessary components for a fully functional EEWRRS, as, for instance, those dedicated to broadcast the alert information or the forecast consequences, are beyond the scope of this article and should be designed considering the end-users' specific requirements.

## Data Layer

### Hazard Model

The hazard model includes the information necessary to populate the scenarios portfolio. In particular a catalog of past events is considered, complemented by location and characteristics of main seismic sources.

As a consequence of the India–Eurasia collision, several strong earthquakes occurred in Central Asia (Kondorskaya *et al.*, 1982), like those that struck the northern Tien-Shan around the end of the nineteenth and the beginning of the twentieth century (1887 M 7.3 Verny earthquake, 1889 M 8.2 Chilik earthquake, 1911 M 8.2 Kemin earthquake, and 1938 M 6.9 Chu-Kemin earthquake). The occurrence of such large earthquakes makes Central Asia one of the areas with the highest earthquake hazard in the world (e.g., Ulomov, 1999). In particular, the seismic hazard estimated from the macroseismic catalog (Bindi *et al.*, 2012) confirmed the intensity corresponding to a 10% probability of exceedance in 50 years ranges between VIII and IX (on the MSK-64 scale) for many large towns in Central Asia (e.g., Almaty, Bishkek, Dushanbe, and Tashkent).

In the case of Bishkek, seismic hazard is controlled by both nearby and distant faults. In particular, the southern edge of Bishkek is bounded by the Issyk-Ata fault, which, on the basis of paleoseismological data, is expected to generate an earthquake of magnitude up to 7.5 (Abdrakhmatov *et al.*, 2003) that would cause serious losses (Bindi *et al.*, 2011; Pittore *et al.*, 2012; Picozzi *et al.*, 2012). Similarly, the 1885 M 6.5 Belovodsk earthquake, which occurred about 50 km west of Bishkek, generated intensity up to VII in the town (see Fig. 2). Con-

sidering that Bishkek currently is the most populous town in Kyrgyzstan, a replica of the Belovodsk earthquake could produce significant damage.

The event portfolio, representative of the main hazard for the considered targets (i.e., Bishkek and Almaty), is composed of a set of 150 scenario earthquakes, depicted in Figure 2. Out of these events, 122 are generated based on the active tectonic fault distribution and background seismicity, whereas 28 events are taken from the historical earthquake database for the region (Bindi *et al.*, 2012).

### Site Effects

The ground-motion simulation should consider the site effects model for the considered target, when available. In the case of Bishkek, local amplification effects have been estimated at 19 different locations within the town, where seismic stations have been installed (Parolai *et al.*, 2010; Ullah *et al.*, 2012; see Fig. 3). The site response is obtained by means of standard spectral ratio (Borcherdt, 1970) between the Fourier spectra of the recordings at the stations located in Bishkek and those of a reference station (Parolai *et al.*, 2010). The site amplifications estimated in this way are affecting a wide frequency band (from nearly 0.2 Hz to a few hertz) and generally increase from south to north (Parolai *et al.*, 2010; Ullah *et al.*, 2012).

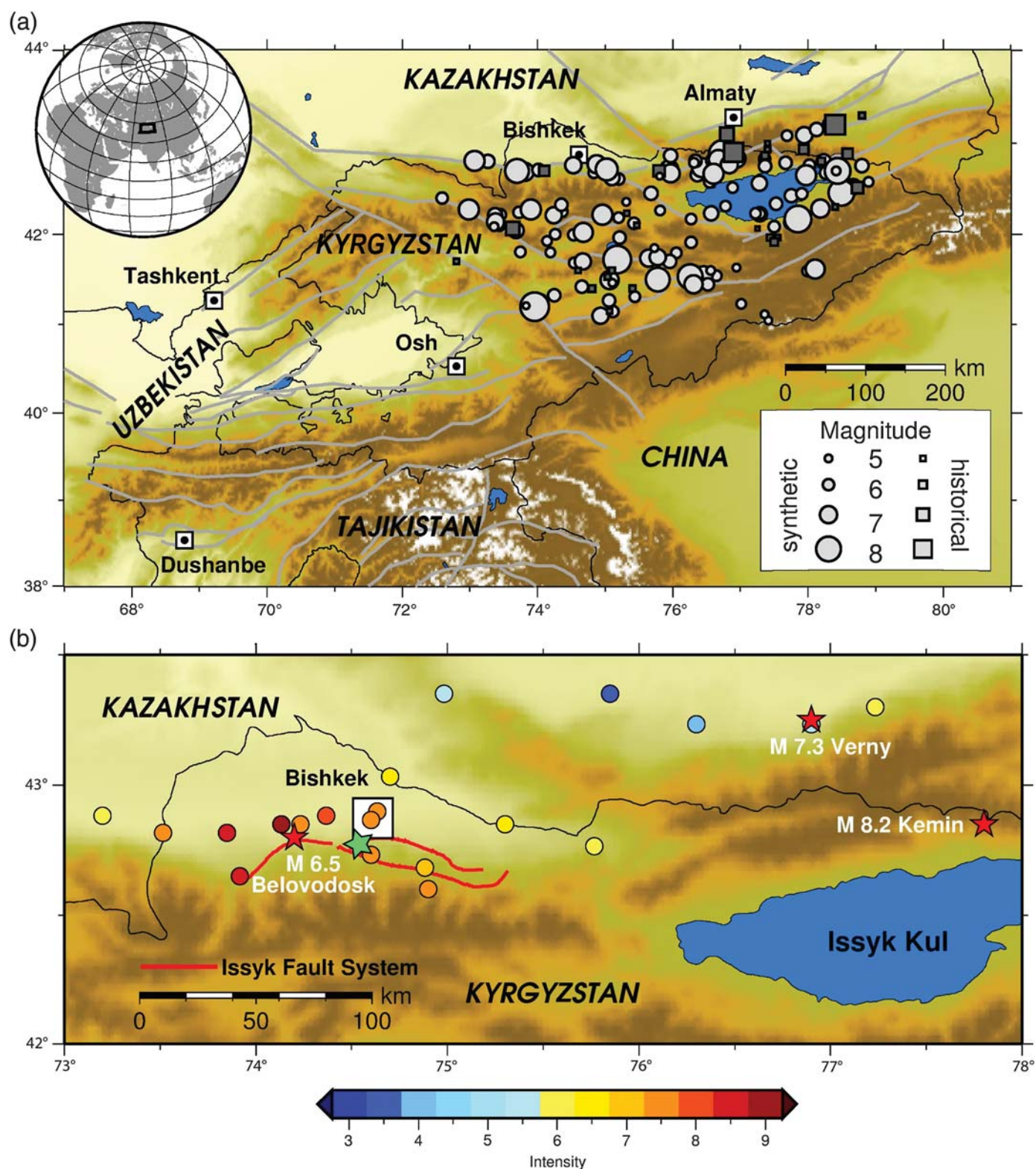
### Exposure/Vulnerability Model

A reliable, spatially resolved exposure model of the considered targets has to be implemented and maintained to estimate the expected loss for each event in the portfolio. The vulnerability model defines the susceptibility to damage the assets contained in the exposure model. The exposure/vulnerability model is based on a two-tier approach (Pittore and Wieland, 2012) that entails a remote sensing-based spatial stratification of the urban environment under study (i.e., the target location of the early warning system) (Wieland *et al.*, 2012) followed by subsequent ground-based vulnerability data collection, either by direct visual assessment or by remote rapid visual screening using mobile mapping systems. The use of mobile mapping systems for local, ground-based data collection provides valuable information about the composition and the characteristics of the exposed assets that would be very difficult to infer solely from spaceborne data, and the use of Bayesian Networks allows efficient integration of expert knowledge and other ancillary information (Pittore and Wieland, 2012) into a probabilistic vulnerability model.

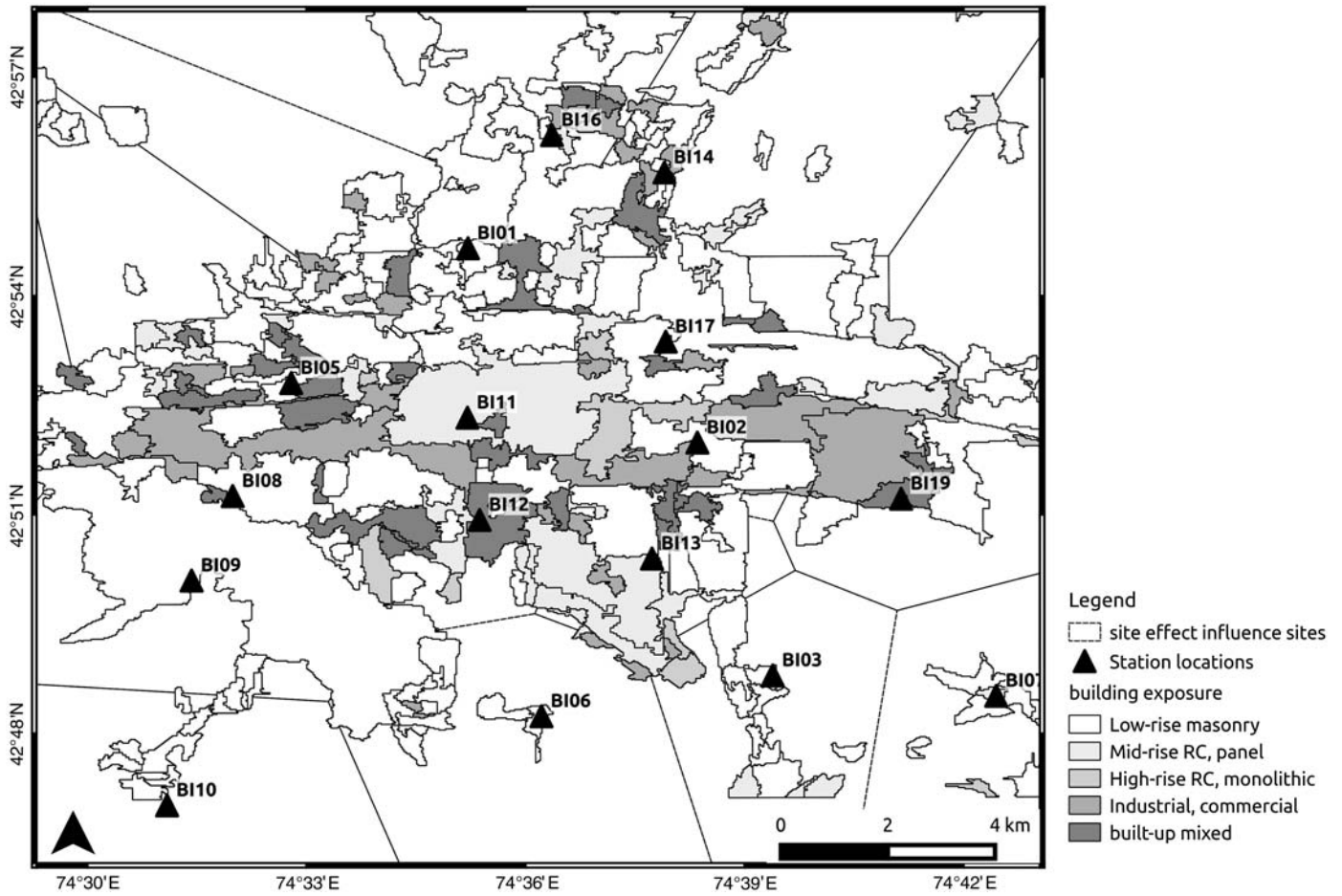
In Figures 3 and 4, the estimated exposure and vulnerability distribution of the town of Bishkek are depicted. The current analysis only considers residential urban buildings stock.

The urban area is subdivided into geocells, for which the distribution of vulnerability has been estimated. We specifically address physical vulnerability, expressed on the European Macroseismic Scale (EMS)-98 (see Grünthal and European Seismological Commission, 1998, p. 98). The EMS-98 classifies the buildings stock into six different vulnerability classes, ranging from class A (most vulnerable) to class F (least vulnerable).





▲ **Figure 2.** (a) Composition of event portfolio used to model the seismic hazard for the towns of Bishkek and Almaty. Circles and squares indicate the location of synthetic and historical earthquakes, respectively. The size of the symbols is proportional to the earthquake's magnitude, and the main active faults are sketched in gray. (b) Location of the intensity assignments (circles) associated to the 1885 M 6.5 Belovodsk earthquake (indicated by a red star) color coded accordingly to their intensity value. The main branches of the Issyk-Ata fault system are shown in red. The green star indicates the location of the scenario event simulated and discussed in this article.



▲ **Figure 3.** Spatial distribution of the residential buildings inventory considered for risk assessment in Bishkek (Kyrgyzstan). The black triangles represent the 19 locations used to estimate site effects and to simulate the expected ground motion.

The map in Figure 4 depicts the average vulnerability of the urban geocells in terms of mean vulnerability index (MVI) defined as

$$\text{MVI}_G = \frac{1}{6n_G} \sum_{b \in G} \left[ \sum_{i=1}^6 v_i p v_i(b) \right], \quad (1)$$

in which the index  $i$  represents the vulnerability levels, in the range from six (equivalent to EMS-98 grade A) to one (equivalent to EMS-98 grade F),  $p v_i(b)$  is the probability of vulnerability state  $v_i$  for each building  $b$ , and  $n_G$  is the number of buildings in the geocell  $G$  (see also Picozzi *et al.*, 2012). In Table 1, a posterior probability distribution for a building for which the following set of evidences applies: mid-rise, built before 1977, belonging to a geocell contained in the geographical stratum 1–2 storeys masonry-brick type 2 (see Pittore and Wieland, 2012). The MVI varies linearly from zero (indicating the maximum level of earthquake resistance) to one (indicating the greatest susceptibility to damages).

Accordingly, for each geocell  $G$ , we can aggregate the values obtained at building level (defined in equation 1 and exemplified in Table 1) and define a vector describing the average

posterior probability of finding a building belonging to vulnerability level  $v_i$ ,  $i = 1, \dots, 6$ :

$$\begin{aligned} p_G(v) &= [\bar{p}_G(v_1), \bar{p}_G(v_2), \dots, \bar{p}_G(v_6)] \\ &= \frac{1}{n_G} \left[ \sum_{b \in G} p v_1(b), \sum_{b \in G} p v_2(b), \dots, \sum_{b \in G} p v_6(b) \right]. \end{aligned} \quad (2)$$

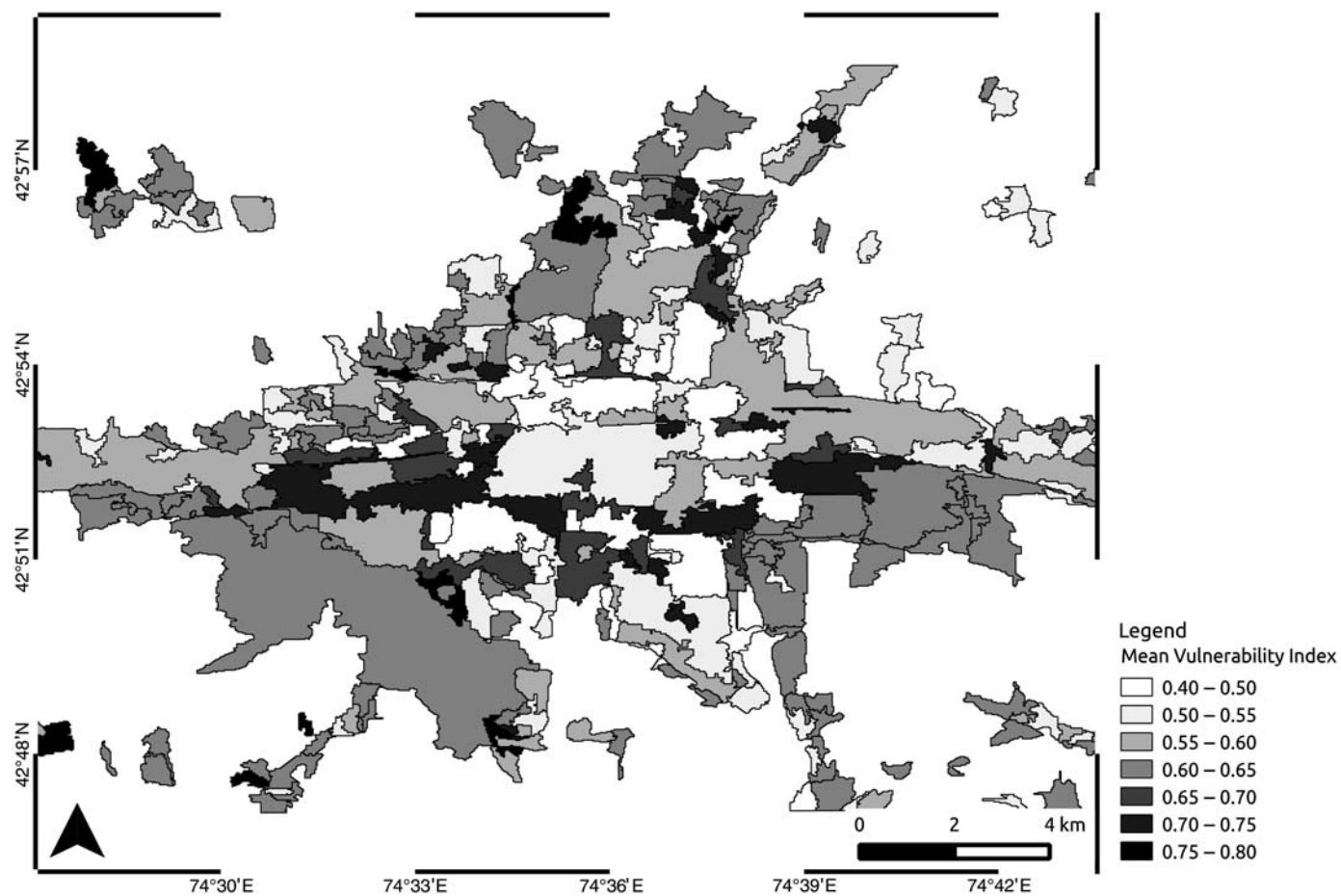
## Optimization and Simulation

### Ground-Motion Engine

To devise the best configuration for the EEWRRS, to evaluate the potential of an already existing system, and also to perform evaluations of expected loss, a comprehensive data set of ground-motion records has to be available. Although records from significant past earthquakes are sparse in Central Asia, we resorted to ground-motion simulations, following previous studies (e.g., Oth *et al.*, 2010; Stankiewicz *et al.*, 2013). In this work, the stochastic finite-fault simulation program EXSIM (Morazedian, 2005) has been used for generating synthetic ground-motion time series.

The software computes the ground acceleration as a function of time at any number of specified locations from a given





▲ **Figure 4.** Distribution of physical vulnerability, in terms of mean vulnerability index, for the residential building stock. The center of the town, dominated by reinforced concrete buildings, is characterized by lower vulnerability with respect to the outskirts, where rapid, often unplanned urbanization takes place.

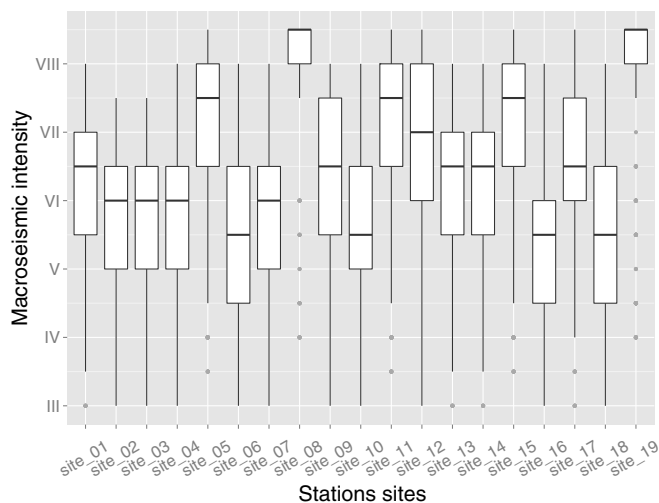
scenario event. The scenario earthquake is defined by moment magnitude, stress parameter, fault length, and dip. Only reverse faulting events were considered in our simulations, in agreement with the dominant source mechanism in the region. When simulating historical events, for which source characterization is often uncertain, simulations were repeated with varying input parameters.

The approach of [Sokolov and Chernov \(1998\)](#), which provides empirical correlation coefficients between earthquake Fourier spectra and macroseismic intensity, has been used to translate the simulated ground motion into intensity. For simulations solely used for the purpose of estimating the intensity

at the target for a given scenario, only the  $S$ -wave component of ground motion was simulated. When complete traces were necessary, such as for trigger-based warning systems, the  $P$ - and  $S$ -wave components were calculated separately using appropriate parameters and added together as described by [Böse et al. \(2009\)](#).

To assign the available site effect estimation, described in [Site Effects](#) section, to spatially distributed vulnerability data, a Voronoi tessellation ([Okabe, 2000](#)) of the urban environment based on the location of the 19 stations has been computed. This was then used to generate by intersection a more refined distribution of the geocells described in [Exposure/Vulnerability Model](#) section. The centers of the Voronoi tessellation (shown in [Fig. 3](#)) were used as reference locations to generate a distribution of macroseismic intensities for each considered scenario. The distribution of macroseismic intensities generated for a portfolio event in the considered locations is shown in [Figure 5](#). The considered seismic event is located on the Issyk-Ata fault, southeast of the Kyrgyzstan capital (see [Fig. 2b](#)), and was assigned a magnitude in the range (7, 7.5). Because all magnitude values in this range are considered equiprobable, the ground-motion engine performs several simulations randomly varying the magnitude in the given range.

<b>Table 1</b> <b>Probability of Vulnerability Level <math>v_i</math> for a Mid-Rise Building in Bishkek</b>					
$pv_1(b)$	$pv_2(b)$	$pv_3(b)$	$pv_4(b)$	$pv_5(b)$	$pv_6(b)$
0.06	0.14	0.08	0.2	0.38	0.14
Building built before 1977 belonging to geographical stratum "1–2 storeys/masonry/type 2."					



▲ **Figure 5.** Distribution of macroseismic intensity resulting from the simulation of an event of magnitude 7 on the Issik-Ata fault, close to Bishkek, in the 19 sites for which local amplification effects have been estimated. The variability in the intensity distribution arises from the uncertainties defined on the earthquake parameters (magnitude and stress drop).

#### Seismic Network Optimization

To achieve optimal performance of an EEWRRS, the seismic network used for this purpose needs to be carefully designed. However, optimal network design is not a straightforward issue. In addition to parameters directly related to seismic risk and damage control, such as the tectonic setting of the area and the location of target cities, parameters limiting the efficiency of the system need to be considered (e.g., available resources, installation, and maintenance costs). In this section, we provide an example of how efficient networks can be designed considering Bishkek as target, finding a balance in the trade-off problem of warnings being simultaneously as timely and accurate as possible.

The process used for evaluating an existing or a hypothetical network is based on the one developed by [Oth et al. \(2010\)](#). Using the synthetic ground-motion database from the event portfolio (see [Scenarios Portfolio](#) section), the effect of each scenario on the target city is considered in terms of the expected peak ground acceleration (PGA). All the events are thus grouped by their expected warning class. Four such classes are defined, including a class 0, in which the PGA does not exceed  $0.02g$  and no warning is necessary. Classes I, II, and III are separated by PGA thresholds of  $0.07$  and  $0.12g$ .

For a given network, the cost (i.e., the value of an objective function defined to evaluate the performance of the system) of each scenario event can be computed using the accuracy of the warning and the available lead time. The network is defined by the locations of a predefined number of stations (typically 10, following [Stankiewicz et al., 2013](#)) and three ground accelerations threshold values. These values are the same for all stations, and although they represent the warning classes, they are not necessarily the same as the thresholds defining the expected

warning class. Instead, they can be thought of a correlation between ground acceleration at the network and at the target. As soon as one of the network threshold levels is exceeded at any three stations, the corresponding warning level is issued at the target. The lead time is defined as the time between this warning and the warning class defining acceleration being experienced at the target. The accuracy of the warning is a simple binary function: was the correct warning class issued?

Finally, the cost value of the entire network is defined as the weighted average of the individual scenario costs. For more information on this methodology and the exact definition of the cost function, we refer the reader to [Oth et al. \(2010\)](#) and [Stankiewicz et al. \(2013\)](#).

Using such a cost function, it is possible to search for optimal network designs (i.e., station locations and trigger thresholds). For solving this nonlinear optimization problem, we resort to genetic algorithms, which consist of a guided search technique based on evolutionary principles ([Stankiewicz et al., 2013](#)).

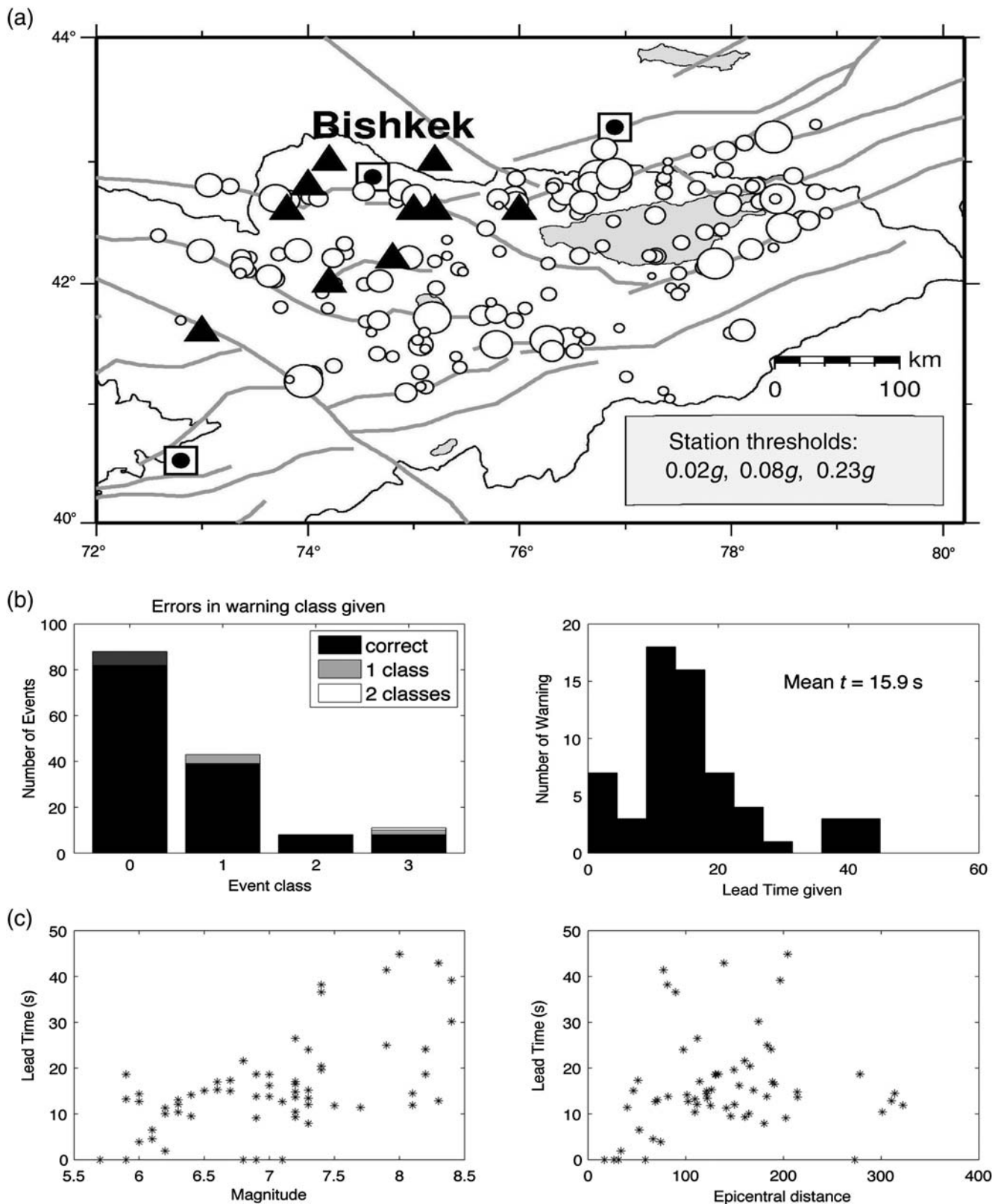
A critical aspect of designing a warning system is finding the balance between warnings being timely and accurate (there is an inherent trade-off between these two conditions). There is no straightforward answer to this question, and this balance must be discussed with the end users of the systems, such as city authorities and rescue teams. For example, it might be considered that lead times less than a few seconds are completely useless. In this case, earthquakes very close to the city would effectively be ignored by the network, which would then be designed for optimal performance in the case of events further away. In [Figure 6](#), an example of a 10-station seismic network is shown, along with the corresponding threshold values at triggering stations, putting the strongest focus on accurate classification.

In contrast, if strongest weight is put on the maximization of lead times, the optimization approach will result in a network configuration that ensures longer lead times but may involve a higher number of false and missed alarms. The optimization process also provides useful insights on the relative importance of the stations with respect to the overall task. In [Figure 7](#), the most selected locations are shown, therefore indicating where efforts should be foreseen to increase the resilience of the network.

#### Risk Engine

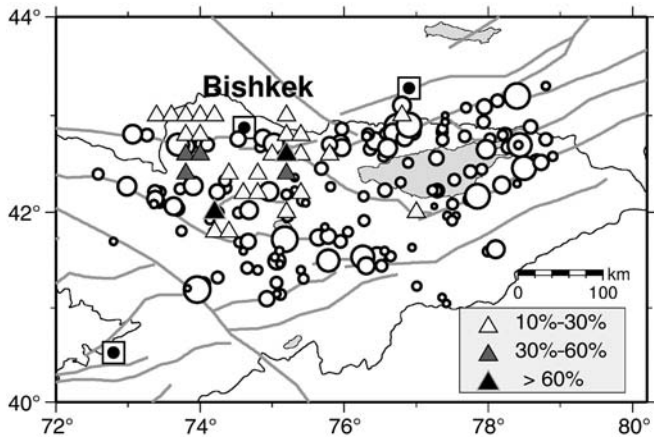
The risk engine component of the proposed system combines the ground motion expected for each event in the portfolio with the exposure/vulnerability model to estimate consequences in terms of probabilistic distribution of damage/loss.

A simple procedure to evaluate expected structural damage is described here, as base for several types of loss assessment (collapses, fatalities and injuries, and economical consequence). For each geocell  $G$ , the module computes the distribution of the probability to given damage state  $d_i$  to be experienced. The damage states  $d_1, \dots, d_5$  represent the five damage states defined by EMS-98, whereas  $d_0$  represents the absence of damage and is explicitly considered to obtain an exhaustive probabilistic description. The damage probability distribution is defined as



▲ **Figure 6.** (a) Arrangement of the seismic stations resulting from the automatic optimization process (and related warning thresholds). Optimization focus was on maximizing the warning accuracy. (b) Left: Distribution of events according to their automatic classification. The number of events misclassified by one or two classes is also indicated. Right: histogram of the resulting lead times when testing this particular configuration with the considered seismic events. (c) Left: distribution of resulting lead time (in seconds) with respect to the event's magnitude. Right: distribution of resulting lead time (in seconds) with respect to the event epicenter's distance from the target (Bishkek).





▲ **Figure 7.** Station locations selected during the optimization process, considering the 1000 solutions with lowest cost function. White triangles indicate locations chosen in 10%–30% of the optimization loops. Gray triangles indicate locations selected between 30% and 60% of the times, whereas black triangles indicate locations chosen in at least 60% of the iterations. Gray and black locations indicate critical locations for optimization given the event portfolio (circles).

$$p_G(d_j) = \sum_{i=1}^6 \left[ p_G(v_i) \sum_{I=V}^X \text{DPM}_{Id}^v p_G(I) \right], \quad (3)$$

in which  $\text{DPM}_{Id}^v$  is the damage probability matrix (DPM) related to vulnerability state  $v$ , which gives the probability of damage state  $d$  resulting from the exposition to intensity  $I$ , and  $p_G(I)$  indicates the probability for the geocell  $G$  to be exposed to macroseismic intensity  $I$  (in EMS-98). The latter is computed from the empirical distributions shown in Figure 5. Macroseismic intensity can vary in the range  $[V, VI, \dots, X]$ , in which DPMs have not null entries. Furthermore,  $p_G(v_i)$  refers to the expected probability to find a building of vulnerability  $v_i$  in the geocell  $G$ , as defined in equation (2).

In Figure 8, several DPMs are shown, for different levels of macroseismic intensity.

The expected distribution of damage is therefore described by the individual probability distributions in the individual cells. To use a single scalar number to simply communicate the expected level of damage, for each geocell the mean damage index (MDI) is computed as

$$\text{MDI}_G = \frac{1}{6} \sum_{i=0}^5 d_i p_G(d_i). \quad (4)$$

## Scenarios Portfolio

### Ground-Motion Scenarios

For each considered scenario event, a distribution of macroseismic intensities (see Fig. 5) is computed by the ground-motion engine for each of the geocells depicted in Figure 3. This set of intensity distributions and the associated seismic event define an element of the ground-motion scenarios portfolio. The portfolio is progressively populated by simulating the events

compatible with the considered hazard model. Moreover, each element of the ground-motion scenarios portfolio has a corresponding element in the risk scenarios portfolio.

### Risk Scenarios

The overall expected loss in terms of MDI is displayed in Figure 9. This is an exemplification of the different risk estimates that would be promptly provided to decision makers along with the warning about the occurrence of the event itself. Once the basic estimates of expected physical damage are computed, several indicators can be computed and provided to further support emergency actions. The uncertainties are considered throughout the loss evaluation process. In Figure 10, three of the loss estimates computed for each geocell are displayed in form of probability of exceedance of EMS-98 damage states, considering the macroseismic intensity distribution as input. It is interesting to note as the distribution of expected damage is strongly influenced by site amplification effects, which are relevant especially in the northern outskirts of the town.

Because most of fatalities are related to the collapse of residential buildings (defined by damages states five on the EMS-98 scale), the locations where more collapses are expected, along with information on the most likely occupancy of the buildings can be used to suitably prioritize operations of search and rescue (S&R) teams.

The resulting risk estimates are stored in the event portfolio, along with the event simulations and the network activation pattern computed in the network optimization phase (see [Seismic Network Optimization](#) section), and will be selected by the scenario identification component (see [Scenario Identification](#) section) in real time. The selected loss scenarios will then be promptly broadcast to interested users.

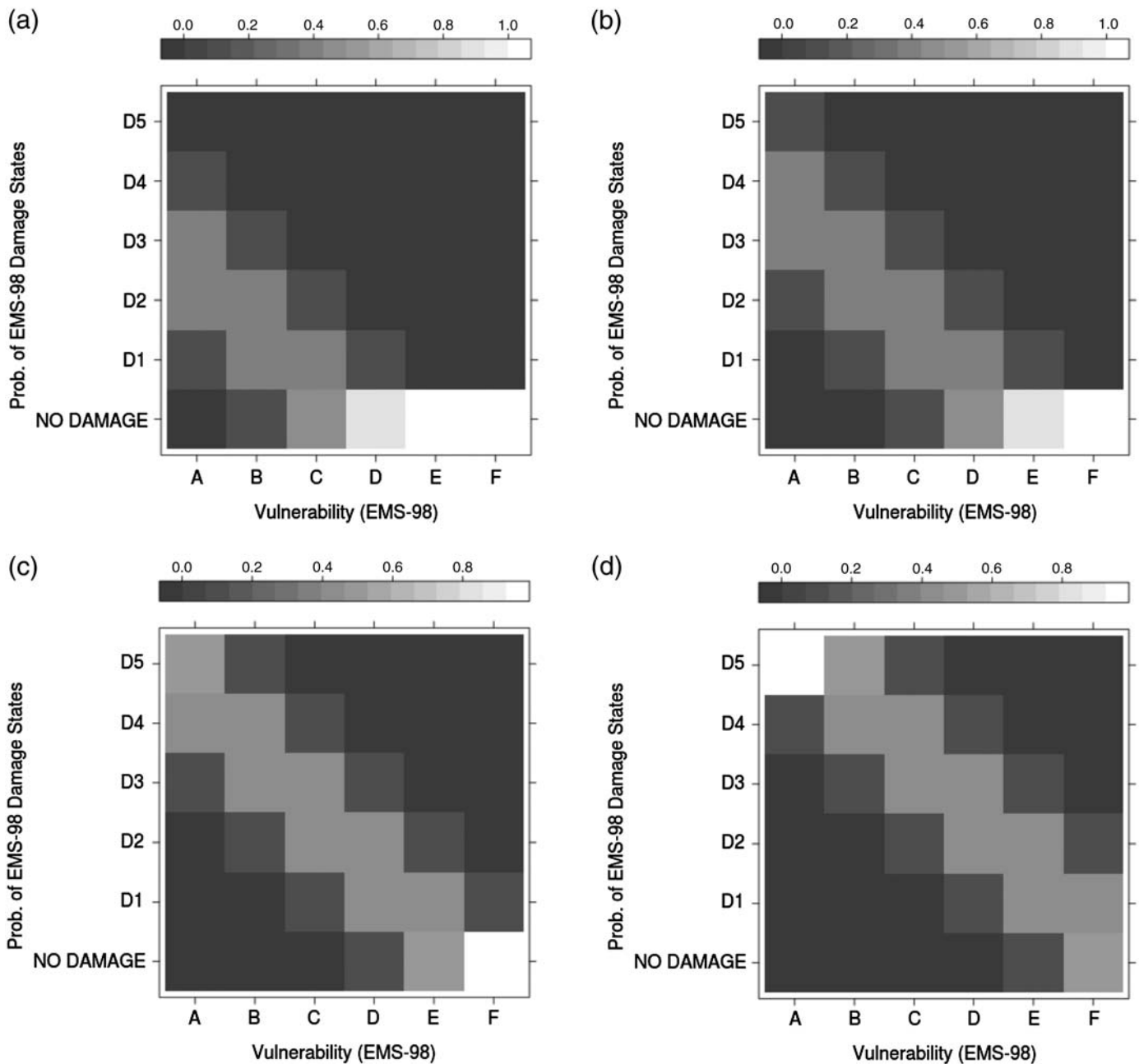
## Real-Time Operations

### Scenario Identification

In the approach used to optimize the station layout and described in [Seismic Network Optimization](#) section, the event detection is based on a set of ground-motion thresholds with consensus activation. Different alert levels (alerts 1, 2, and 3) are defined to provide decision makers with simple warning information. Alert 1 represents a simple event trigger (an earthquake has been detected, but no strong ground shaking is expected at the target site), whereas alerts 2 and 3 indicate levels of ground shaking that would be dangerous for the target site. The alert levels and relative triggers thresholds can be automatically selected either considering the distribution of ground motion at target or based on the computed loss scenarios.

The system proposed focuses on rapid dissemination of loss estimates. Therefore, in parallel to the threshold approach, the real-time data streams from the regional EEW network are processed according to the following scheme:

1. A trigger algorithm based on standard short-term/long-term averages; the occurrence of an earthquake is declared when at least three stations triggered.
2. Using the equal differential time evolutionary approach ([Satriano et al., 2008](#)), the location procedure starts when



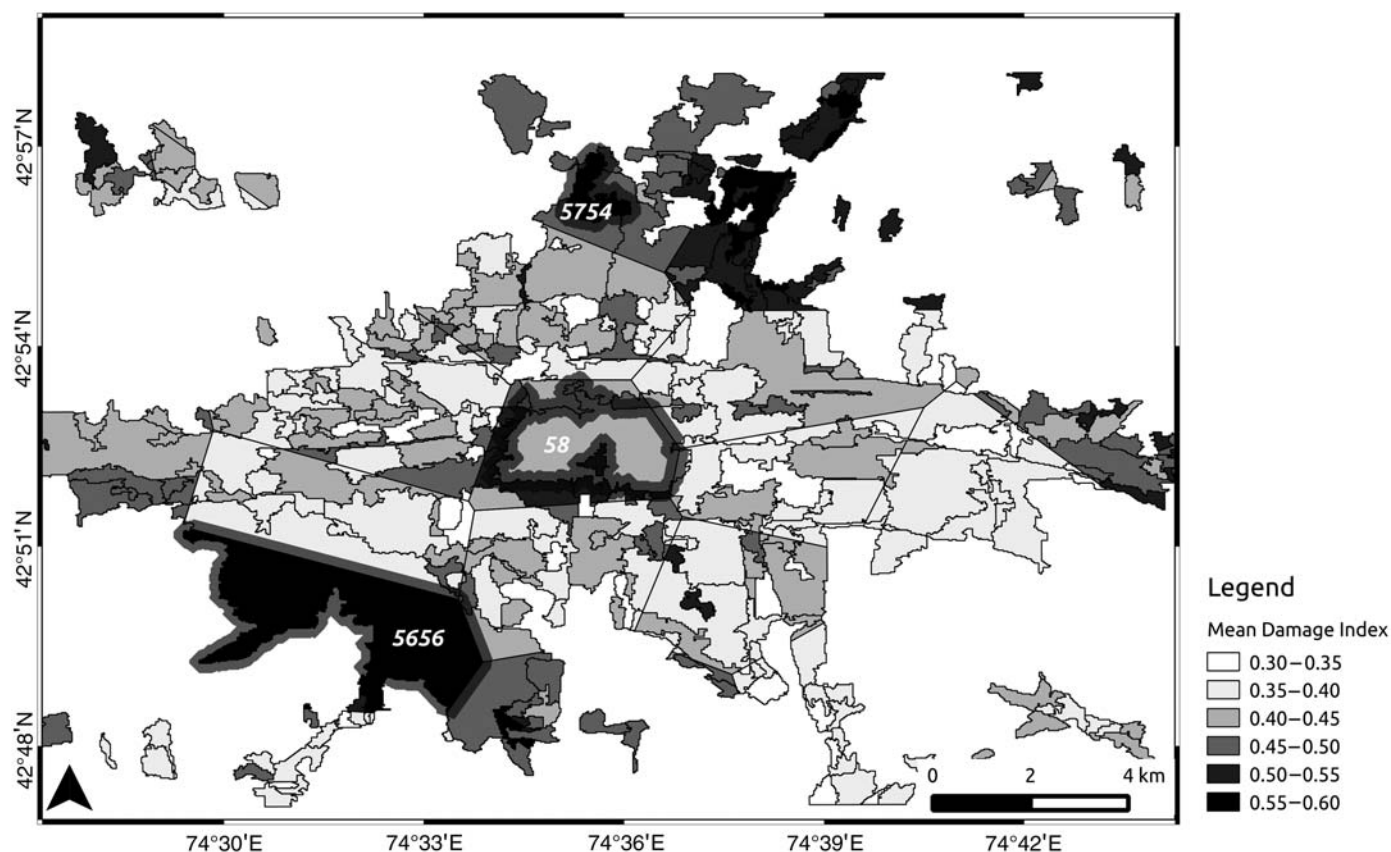
▲ **Figure 8.** Damage probability matrices computed following the [Giovinazzi and Lagomarsino \(2004\)](#) approach, corresponding to different levels of macroseismic intensity. (a) VII, (b) VIII, (c) IX, and (d) X. We can note, for instance, that at intensity  $I = X$ , a complete destruction of building of vulnerability class A is expected.

the first station is triggered and then refined with new incoming triggers; the magnitude of the event is estimated from proxies, for example, the peak displacement ([Allen and Kanamori, 2003](#)).

3. The estimated location and source are used to restrict the set of suitable candidates in the scenario portfolio;  $P$ -wave spectral comparison at triggered stations with selected scenarios is performed to refine the scenario selection; the expected losses at the target location relevant to the selected scenario are evaluated and decision taken, according to the expected damage and loss distributions. Among the

candidate scenarios, the most compatible and the worst case are provided to end users and decision makers to streamline the management of the incoming emergency. The scenario selection could further be improved by the use of Bayesian updating or other probabilistic approaches ([Iervolino et al., 2006](#)).

In the operational stage, depending on the alert level and the approximate location of the event, a loss scenario is then chosen from the scenarios portfolio following the above-described steps and promptly forwarded to end users.



▲ **Figure 9.** Expected distribution of damage related to an event of magnitude ranging from 7 to 7.5 on Issyk-Ata fault, near Bishkek (Kyrgyzstan). The location of the event is shown in Figure 2. Three individual geocells are highlighted, marked by their ID value.

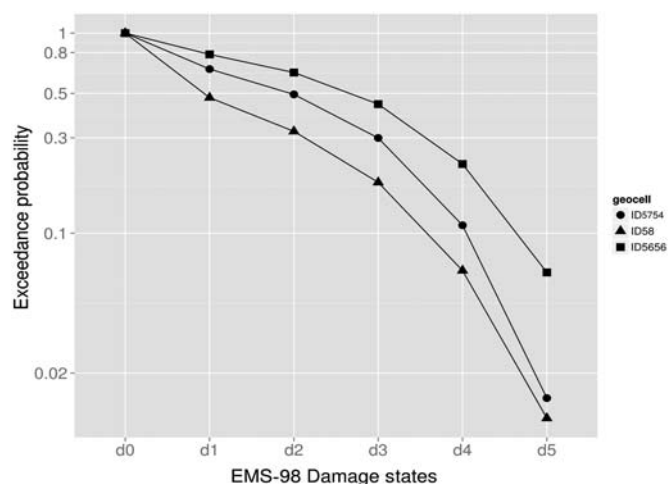
#### Seismic Monitoring Network

The monitoring network is composed by several seismic stations geographically distributed around the considered target. The stations operate in real time and are permanently linked to a data collection center, where the digital data are collected and proc-

essed. The spatial arrangement of the stations is determined by the seismic network optimization described in [Seismic Network Optimization](#) section. The specific characteristics of the stations and the data link are to be determined case by case.

#### On-Site Monitoring Network

The proposed system's architecture would also greatly benefit from the use of locally deployed, distributed networks of low-cost seismic monitoring devices, which could provide real-time ground-shaking information and be integrated as an on-site EEW system component. Self-Organizing Seismic Early Warning Information Network (SOSEWIN) instruments have been already tested in Turkey and Central Asia ([Fleming et al., 2009](#)) and would prove useful to provide a prompt validation of the expected macroseismic intensity distribution estimated by the scenario identification component. This would in turn allow for a rapid calibration of the loss scenario selected by the system, with a consequent increase of the reliability of the estimates. Moreover, such distributed sensor networks could be used to assess structural performance of affected buildings (e.g., schools or hospitals) by providing *in situ*, automatic and real-time damage assessment, and building height monitoring. The installation of such a monitoring network is currently ongoing in Bishkek, and its effective performance will be extensively validated.



▲ **Figure 10.** Three exceeding probability of damage for a single scenario (M 7 event on Issik-Ata fault). The considered geocells are the same as those highlighted in Figure 8.



## CONCLUSIONS, CHALLENGES, AND FUTURE OUTLOOK


EEW systems have been called upon to protect communities from the threat of one of the most unpredictable and potentially damaging natural hazards, especially in those countries more exposed and less capable of significant investments. Yet, despite the capabilities of modern engineering seismology, only a few countries have been able to implement a fully operational EEW systems. Often (as is the case in Central Asia) a hybrid approach, in which on-site early warning and rapid response is additionally considered to broaden the scope and usefulness of EEW systems, while also strongly improving their cost-benefit ratio. The inherent challenges are severe and complex, but the benefits can largely overcome the limitations, provided that a pragmatic stance is taken and strong efforts to optimize the design and development of such systems are pursued.

An efficient EEWRSS's architecture is laid out in this article, which would provide a sound platform both for timely and useful warning and for improving the efficiency of emergency management. Among the key points of this framework, we can mention the integrated, uncertainty aware risk assessment, the use of simulated event portfolio, and the loss-driven optimization of the real-time monitoring network.

Including a thorough evaluation of vulnerability and risk of the target site would increase the general awareness of the exposed communities, thus helping to focus further resources to prevention and mitigation. It is worthwhile noting that even if based on a rapid assessment of seismic exposure and vulnerability, mostly based on medium-resolution satellite imagery, the computed loss estimates are spatially defined with a resolution already suitable to support both prevention and mitigation actions and emergency operations. Explicitly, considering the uncertainties beneath the risk assessment allows for a more reliable and robust framework for communicating risk to decision makers and risk practitioners. Moreover, the provision of reliable loss estimates at the warning stage would help practitioners to improve the management of the emergency, for example, by optimizing the deployment of S&R operations.

The development of a scenario events portfolio, compatible with the local hazard conditions, introduces a scenario-based risk analysis, which provides sound estimates of the expected amount and distribution of loss, in which site amplification effects can be readily integrated. Furthermore, the use of optimization algorithms to define the optimal spatial arrangement of seismic monitoring stations, driven by a user-defined cost function, provides an intuitive and flexible way to account for many different factors, including available resources and installation constraints, but more importantly also allows specifying the priorities of the deployed system in terms of alerting performance.

The road map for next generation EEW systems, particularly in Central Asia, is just drawn and much still has to be done, from the scientific and technological standpoint, but flexible, affordable, and efficient EEW systems might be of critical importance in the near future to successfully mitigate the

social and economic consequences of seismic events and to raise seismic risk awareness in the endangered communities. 

## ACKNOWLEDGMENTS

This work was supported by PROGRESS (Georisiken im Globalen Wandel), Earthquake Model Central Asia (EMCA), REAKT (Strategies and tools for Real-time EArthquake risk reducTion), and SENSUM (Framework to integrate Space-based and *in situ* sENSing for dynamic vULnerability and recovery Monitoring, Grant agreement Number 312972). Support was also provided by the Fonds National de la Recherche, Luxembourg, cofunded by the Marie Curie Actions (project 4817114).

## REFERENCES

- Abdrakhmatov, K., H.-B. Havenith, D. Delvaux, D. Jongmans, and P. Trefois (2003). Probabilistic PGA and arias intensity maps of Kyrgyzstan (Central Asia), *J. Seismol.* **7**, 203–220, doi: [10.1023/A:1023559932255](https://doi.org/10.1023/A:1023559932255).
- Allen, R. M., and H. Kanamori (2003). The potential for earthquake early warning in southern California, *Science* **300**, 786–789, doi: [10.1126/science.1080912](https://doi.org/10.1126/science.1080912).
- Astoul, A., C. Filliter, E. Mason, A. Rau-Chaplin, K. Shridhar, B. Varghese, and N. Varshney (2013). Developing and testing the automated post-event earthquake loss estimation and visualisation (APE-ELEV) technique, *Bull. Earthq. Eng.* **11**, 1973–2005, doi: [10.1007/s10518-013-9495-7](https://doi.org/10.1007/s10518-013-9495-7).
- Bindi, D., K. Abdrakhmatov, S. Parolai, M. Mucciarelli, G. Grünthal, A. Ischuk, N. Mikhailova, and J. Zschau (2012). Seismic hazard assessment in Central Asia: Outcomes from a site approach, *Soil Dynam. Earthq. Eng.* **37**, 84–91, doi: [10.1016/j.soildyn.2012.01.016](https://doi.org/10.1016/j.soildyn.2012.01.016).
- Bindi, D., M. Mayfield, S. Parolai, S. Tyagunov, U. T. Begaliev, K. Abdrakhmatov, B. Moldobekov, and J. Zschau (2011). Towards an improved seismic risk scenario for Bishkek, Kyrgyz Republic, *Soil Dynam. Earthq. Eng.* **31**, 521–525, doi: [10.1016/j.soildyn.2010.08.009](https://doi.org/10.1016/j.soildyn.2010.08.009).
- Borcherdt, R. D. (1970). Effects of local geology on ground motion near San Francisco Bay, *Bull. Seismol. Soc. Am.* **60**, no. 1, 29–61.
- Böse, M., E. Hauksson, K. Solanki, H. Kanamori, Y.-M. Wu, and T. H. Heaton (2009). A new trigger criterion for improved real-time performance of onsite earthquake early warning in southern California, *Bull. Seismol. Soc. Am.* **99**, 897–905, doi: [10.1785/0120080034](https://doi.org/10.1785/0120080034).
- Erdik, M., N. Aydinoglu, Y. Fahjan, K. Sesetyan, M. Demircioglu, B. Siyahi, E. Durukal, C. Ozbey, Y. Biro, and H. Akman (2003). Earthquake risk assessment for Istanbul metropolitan area, *Earthq. Eng. Eng. Vib.* **2**, 1–23.
- Espinosa-Aranda, J. M., A. Cuéllar, F. H. Rodríguez, B. Frontana, G. Ibarrola, R. Islas, and A. García (2011). The seismic alert system of Mexico (SASMEX): Progress and its current applications, *Soil Dynam. Earthq. Eng.* **31**, 154–162, doi: [10.1016/j.soildyn.2010.09.011](https://doi.org/10.1016/j.soildyn.2010.09.011).
- Fleming, K., M. Picozzi, C. Milkereit, F. Kühnlenz, B. Lichtblau, J. Fischer, C. Zulfikar, O. Özel, and the SAFER and EDIM working groups (2009). The self-organizing seismic early warning information network (SOSEWIN), *Seismol. Res. Lett.* **80**, 755–771, doi: [10.1785/gssrl.80.5.755](https://doi.org/10.1785/gssrl.80.5.755).
- Giovinazzi, S., and S. Lagomarsino (2004). A macroseismic method for the vulnerability assessment of buildings, in *13th World Conference on Earthquake Engineering*, Vancouver, British Columbia, Canada, 1–6 August 2004, Paper No. 896.
- Grünthal, G., and European Seismological Commission (1998). European macroseismic scale 1998: EMS-98: Luxembourg, European Seismological Commission Subcommission on Engineering Seismology Working Group Macroseismic scales.

- Horiuchi, S., H. Negishi, K. Abe, A. Kamimura, and Y. Fujinawa (2005). An automatic processing system for broadcasting earthquake alarms, *Bull. Seismol. Soc. Am.* **95**, 708–718, doi: [10.1785/0120030133](https://doi.org/10.1785/0120030133).
- Iervolino, I., V. Convertito, M. Giorgio, G. Manfredi, and A. Zollo (2006). Real-time risk analysis for hybrid earthquake early warning system, *J. Earthq. Eng.* **10**, 867–885, doi: [10.1080/13632460609350621](https://doi.org/10.1080/13632460609350621).
- Kircher, C. A., R. V. Whitman, and W. T. Holmes (2006). HAZUS earthquake loss estimation methods, *Nat. Hazards Rev.* **7**, 45–59, doi: [10.1061/\(ASCE\)1527-6988\(2006\)7:2\(45\)](https://doi.org/10.1061/(ASCE)1527-6988(2006)7:2(45)).
- Kondorskaya, N. V., N. V. Shebalin, Y. A. Khrometskaya, and A. D. Gvishiani (1982). New catalog of strong earthquakes in the USSR from ancient times through 1977, *Report SE-31*, World Data Center A for Solid Earth Geophysics, Washington, D.C.
- Lee, W. H. K., and J. M. Espinosa-Aranda (2002). Earthquake early warning systems: Current status and perspectives, in *Early Warning Systems for Natural Disaster Reduction*, Springer-Verlag, Springer, Berlin, Heidelberg.
- Molina, S., D. H. Lang, C. D. Lindholm, and F. Lingvall (2010). *User Manual for the Earthquake Loss Estimation Tool: SELENA (v5. 0)*, <http://selena.sourceforge.net/selenamanual.pdf> (last accessed September 2014).
- Motazedian, D. (2005). Stochastic finite-fault modeling based on a dynamic corner frequency, *Bull. Seismol. Soc. Am.* **95**, 995–1010, doi: [10.1785/0120030207](https://doi.org/10.1785/0120030207).
- Nakamura, Y. (2004). UrEDAS, urgent earthquake detection and alarm system, now and future, in *Proc. of the 13th World Conference on Earthquake Engineering*, Vancouver, British Columbia, Canada, 1–6 August 2004, Paper No. 908.
- Okabe, A. (2000). *Spatial Tessellations: Concepts and Applications of Voronoi Diagrams*, Wiley, Chichester, New York, 671 pp.
- Oth, A., M. Böse, F. Wenzel, N. Köhler, and M. Erdik (2010). Evaluation and optimization of seismic networks and algorithms for earthquake early warning—The case of Istanbul (Turkey), *J. Geophys. Res.* **115**, doi: [10.1029/2010JB007447](https://doi.org/10.1029/2010JB007447).
- Parolai, S., S. Orunbaev, D. Bindi, A. Strollo, S. Usupaev, M. Picozzi, D. Di Giacomo, P. Augliera, E. D'Alema, C. Milkereit, B. Moldobekov, and J. Zschau (2010). Site effects assessment in Bishkek (Kyrgyzstan) using earthquake and noise recording data, *Bull. Seismol. Soc. Am.* **100**, 3068–3082, doi: [10.1785/0120100044](https://doi.org/10.1785/0120100044).
- Picozzi, M., D. Bindi, M. Pittore, K. Kielling, and S. Parolai (2012). Real-time risk assessment in seismic early warning and rapid response: A feasibility study in Bishkek (Kyrgyzstan), *J. Seismol.* **17**, no. 2, 485–505, doi: [10.1007/s10950-012-9332-5](https://doi.org/10.1007/s10950-012-9332-5).
- Pittore, M., and M. Wieland (2012). Toward a rapid probabilistic seismic vulnerability assessment using satellite and ground-based remote sensing, *Nat. Hazards* **68**, no. 1, 115–145, doi: [10.1007/s11069-012-0475-z](https://doi.org/10.1007/s11069-012-0475-z).
- Pittore, M., D. Bindi, K. Fleming, S. Parolai, M. Picozzi, M. Pilz, J. Stankiewicz, S. Tyagunov, S. Ullah, M. Wieland, and J. Zschau (2012). Seismic risk assessment for earthquake early warning and rapid response systems: The Bishkek (Kyrgyzstan) test case, in *Proc. of the XXIII European Seismological Commission*, Moscow, Russia, 19–24 August 2012.
- Robinson, D., T. Dhu, and J. Schneider (2006). Practical probabilistic seismic risk analysis: A demonstration of capability, *Seismol. Res. Lett.* **77**, 453–459, doi: [10.1785/gssrl.77.4.453](https://doi.org/10.1785/gssrl.77.4.453).
- Saita, J., T. Sato, and Y. Nakamura (2008). What is the useful application of the earthquake early warning system? in *The 14th World Conference on Earthquake Engineering*, Beijing, China, 12–17 October 2008.
- Satriano, C., A. Lomax, and A. Zollo (2008). Real-time evolutionary earthquake location for seismic early warning, *Bull. Seismol. Soc. Am.* **98**, 1482–1494, doi: [10.1785/0120060159](https://doi.org/10.1785/0120060159).
- Sokolov, V. Y., and Y. K. Chernov (1998). On the correlation of seismic intensity with Fourier amplitude spectra, *Earthq. Spectra* **14**, 679–694, doi: [10.1193/1.1586022](https://doi.org/10.1193/1.1586022).
- Sousa, M. L., A. Campos Costa, A. Carvalho, and E. Coelho (2004). An automatic seismic scenario loss methodology integrated on a geographic information system, in *Proc. of the 13th World Conference on Earthquake Engineering*, Vancouver, Canada, 1–6 August 2004.
- Stankiewicz, J., D. Bindi, A. Oth, and S. Parolai (2013). Designing efficient earthquake early warning systems: Case study of Almaty, Kazakhstan, *J. Seismol.* **17**, 1125–1137, doi: [10.1007/s10950-013-9381-4](https://doi.org/10.1007/s10950-013-9381-4).
- Ullah, S., D. Bindi, M. Pittore, M. Pilz, S. Orunbaev, B. Moldobekov, and S. Parolai (2012). Improving the spatial resolution of ground motion variability using earthquake and seismic noise data: The example of Bishkek (Kyrgyzstan), *Bull. Earthq. Eng.* **11**, no. 2, 385–399, doi: [10.1007/s10518-012-9401-8](https://doi.org/10.1007/s10518-012-9401-8).
- Ulomov, V. I. (1999). Seismic hazard of Northern Eurasia, *Ann. Geophys.* **42**, 1023–1038.
- Wald, D. J., K. Jaiswal, K. D. Marano, D. B. Bausch, and M. G. Hearne (2010). PAGER—Rapid assessment of an earthquake's impact, *U.S. Geol. Surv. Fact Sheet*.
- Wenzel, F., and D. Lungu (2000). Earthquake risk assessment for Romania, *EuroConference on Global Change and Catastrophic Risk Management, Earthquake Risks in Europe, ILASA*, Laxenburg, Austria, 6–9 July 2000.
- Wenzel, F., and J. Zschau (2014). *Early Warning for Geological Disasters: Scientific Methods and Current Practice*, Springer, New York, New York, ISBN: 978-3-642-12232-3 (Print) and 978-3-642-12233-0 (Online).
- Wieland, M., M. Pittore, S. Parolai, J. Zschau, B. Moldobekov, and U. Begaliev (2012). Estimating building inventory for rapid seismic vulnerability assessment: Towards an integrated approach based on multi-source imaging, *Soil Dynam. Earthq. Eng.* **36**, 70–83, doi: [10.1016/j.soildyn.2012.01.003](https://doi.org/10.1016/j.soildyn.2012.01.003).
- Wu, Y.-M., N.-C. Hsiao, W. H. Lee, T. Teng, and T.-C. Shin (2007). State of the art and progress in the earthquake early warning system in Taiwan, in *Earthquake Early Warning Systems*, Springer, Springer, Berlin, Heidelberg, 283–306, ISBN: 978-3-540-72241-0.

M. Pittore  
D. Bindi  
M. Wieland  
T. Boxberger  
S. Parolai

GFZ German Research Centre for Geosciences  
Helmholtz Centre Potsdam  
Helmholtzstraße 7  
D-14467 Potsdam, Germany  
[pittore@gfz-potsdam.de](mailto:pittore@gfz-potsdam.de)

J. Stankiewicz  
A. Oth

European Center for Geodynamics and Seismology  
Rue Josy Welter 19  
L-7256 Walferdange, Luxembourg